

NUMERICAL MODELLING OF THE RECOIL OF A POROUS CYLINDER FROM  
A RIGID OBSTACLE

S. P. Kiselev, V. M. Fomin, and Yu. A. Shitov

UDC 539.3

The recoil of a continuous cylinder (impactor) from a nondeformable obstacle was studied by many authors ([1-4], for example). The recoil of a porous impactor from a rigid obstacle is investigated in this paper. It is shown that the contact time and the nature of the pore filling depend on the ratio between the impactor length and its radius.

1. The behavior of a porous body is described within the framework of the Prandtl-Reiss model [5]. The presence of pores in the impactor is taken into account by selecting the equation of state that will be presented below. Such an approach is valid for sufficiently intensive loads when complete pore filling occurs in the plastic shockwave front. In a two-dimensional formulation the Prandtl-Reiss equations have the form [4-6]

$$\begin{aligned} \frac{\partial \rho}{\partial t} + \rho \left( \frac{\partial u}{\partial r} + \frac{\partial w}{\partial z} + k \frac{u}{r} \right) &= 0, \\ \rho \frac{\partial u}{\partial t} &= -\frac{\partial p}{\partial r} + \frac{\partial S_{rr}}{\partial r} + \frac{\partial S_{rz}}{\partial z} + k \frac{S_{rr} - S_{\varphi\varphi}}{r}, \\ \rho \frac{\partial w}{\partial t} &= -\frac{\partial p}{\partial z} + \frac{\partial S_{rz}}{\partial r} + \frac{\partial S_{zz}}{\partial z} + k \frac{S_{rz}}{r}, \frac{\partial r}{\partial t} = u, \frac{\partial z}{\partial t} = w, \\ \frac{\partial S_{rr}}{\partial t} &= 2\mu \left( \frac{\partial u}{\partial r} + \frac{1}{3\rho} \frac{\partial \rho}{\partial t} \right), \frac{\partial S_{zz}}{\partial t} = 2\mu \left( \frac{\partial w}{\partial z} + \frac{1}{3\rho} \frac{\partial \rho}{\partial t} \right), \\ \frac{\partial S_{\varphi\varphi}}{\partial t} &= 2\mu \left( k \frac{u}{r} + \frac{1}{3\rho} \frac{\partial \rho}{\partial t} \right), \frac{\partial S_{rz}}{\partial t} = \mu \left( \frac{\partial u}{\partial z} + \frac{\partial w}{\partial r} \right), \\ \sigma_{ij} &= -p\delta_{ij} + S_{ij} \quad (i, j = 1, 2, 3), S_{rr}^2 + S_{zz}^2 + S_{\varphi\varphi}^2 + 2S_{rz}^2 \leq \frac{2}{3} Y^2, \end{aligned} \quad (1.1)$$

where  $\rho$  is the density;  $u, w$  are the velocity vector components along  $r$  and  $z$ ;  $p$  is the pressure;  $\sigma_{ij}, S_{ij}$  are stress tensor and stress deviator components,  $Y$  is the yield point,  $\mu$  is the shear modulus, and  $k = 0$  corresponds to the plane and  $k = 1$  to the axisymmetric case. The system (1.1) is closed by the equation of state

$$p = p(\rho, m_2), \quad \rho = \rho_s m_2, \quad m_1 + m_2 = 1 \quad (1.2)$$

( $\rho, \rho_s$  are the density of the porous and continuous bodies,  $m_2, m_1$  are the volume concentrations of the continuous body and the pore). To select the equation of state, we use the shock adiabat equation presented in [7], for example. According to [7], pore filling starts in the plastic domain upon satisfaction of the condition

$$p > p_0, \quad p_0 = -(2/3)Y \ln(1 - m_2^0), \quad m_2^0 = 1 - m_1^0 \quad (1.3)$$

( $m_1^0$  is the initial porosity). For the pressure  $p < p_0$  pore filling does not occur, consequently

$$p = c_0^2(\rho_s - \rho_s^0) + \Gamma\rho\varepsilon, \quad m_2 = 0, \quad m_2 = m_2^0 \quad (1.4)$$

( $\Gamma$  is the Grüneisen coefficient). Equations (1.4) are supplemented by the equation for the internal energy  $\varepsilon$

$$\frac{\partial \varepsilon}{\partial t} = \frac{p}{\rho^2} \frac{\partial \rho}{\partial t} + \frac{1}{\rho} \left( S_{rr} \frac{\partial u}{\partial r} + S_{zz} \frac{\partial w}{\partial z} + S_{rz} \left( \frac{\partial u}{\partial z} + \frac{\partial w}{\partial r} \right) + k S_{\varphi\varphi} \frac{u}{r} \right). \quad (1.5)$$

The domain of applicability of (1.4) and (1.5) is shown by the number 1 in Fig. 1. The change in pore volume because of elastic unloading in the pores is neglected in (1.4). After  $p$  has exceeded  $p_0$ , plastic filling of the pores occurs. This domain is denoted by the number 2 in Fig. 1. We will consider the density of the solid body constant

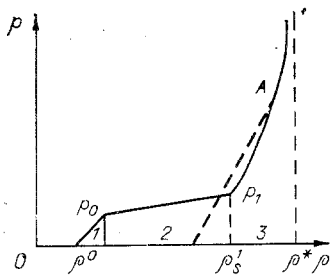


Fig. 1

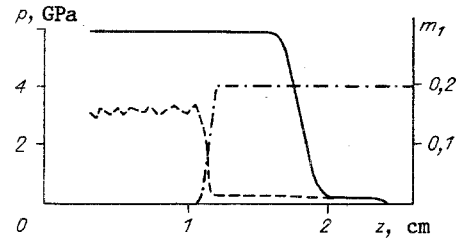


Fig. 2

$$\rho_s = \rho_s^1 = \text{const}, m_2^0 < m_2 < 1, \quad (1.6)$$

where  $\rho_s^1$  is found from (1.4) under the condition  $p = p_0$ . We take the dependence of the pressure on the mean density in the form

$$p = p_0(1 + \beta(\rho - \rho_1)), \quad \rho_1 = m_2^0 \rho_s^1. \quad (1.7)$$

Here  $\beta$  is calculated from the formula  $p_1 = p_0(1 + \beta(\rho_s^1 - \rho_1))$ , and  $p_1$  from the shock adiabat. Let us note that in the case when incomplete filling of the pores plays a substantial part, the more exact equation (20) from [7] must be used in place of (1.7). The shock adiabat for complete filling of the pores is determined in [7-9] and has the form

$$\begin{aligned} p(m_2^0, \rho) &= (\rho_s^0 c_0^2 (v_1(h+1) - v_1^2 h / m_2^0 - m_2^0) + \\ &+ (1-h)(v_1 - m_2^0) p_0 / m_2^0 + p_0(h - v_1)) / (h v_1 - 1), \\ \rho_s^1 &< \rho < \rho^*, \quad \rho^* = h \rho^0, \quad v_1 = \rho^0 / \rho, \\ \rho^0 &= m_2^0 \rho_s^0, \quad m_2 = 1, \quad h = 1 + 2/\Gamma. \end{aligned} \quad (1.8)$$

The domain of applicability of (1.8) is shown by the number 3 in Fig. 1. Unloading from the state A occurs according to an adiabetic law (the appropriate adiabat is given by dashed lines).

The solution of the system (1.1)-(1.8) was performed numerically by the Wilkins method [5].

2. To clarify the singularities of shockwave propagation in a porous body the one-dimensional plane problem of a piston is considered. We assume that a nondeformable piston starts to move in a solid body at the constant velocity  $w_0$ . Then an elastic-plastic wave starts to move ahead of the piston while a uniaxial-strain state is realized behind its front. Assuming all the functions in (1.1) dependent on  $z$ ,  $k = 0$ ,  $u = 0$ , and  $\partial u / \partial z = 0$ , we obtain a one-dimensional system of equations that is closed by the conditions (1.2)-(1.8). We give the initial conditions in the form  $w = 0$ ,  $\sigma_{ij} = 0$ ,  $\rho_s = \rho_s^0$ ,  $m_2 = m_2^0$ , and the boundary condition  $w = w_0$ . We select as parameters  $w_0 = 10^3$  m/sec,  $\rho_s^0 = 10^3$  kg/m<sup>3</sup>,  $c_0 = 5 \cdot 10^3$  m/sec,  $\Gamma = 1.18$ ,  $\mu = 25$  GPa,  $Y = 0.3$  GPa. The porous ( $m_2^0 = 0.8$ ) and the continuous ( $m_2^0 = 1$ ) materials are computed for these parameters.

The pressure  $p(z)$  and porosity  $m_2(z)$  distributions at the time  $t = 3$   $\mu$ sec are presented in Fig. 2. The solid line is  $p(z)$  in the continuous body, the dashes in the porous, and the dash-dot is  $m_2(z)$ . It follows from Fig. 2 that the pressure behind the plastic wave front in the continuous body is twice the pressure in the porous body while the corresponding plastic wave velocity is 1.63 times greater. Complete filling of the pores occurs in the plastic wave front. The elastic forerunner in the continuous and porous bodies is

TABLE 1

$w_0$ , m/sec	$m_x^0$ impactor				
	short			long	
	0,8	0,9	1,0	0,9	1,0
300	1,4	1,4	0,92	15,3	14,5
400	1,5	1,32	0,91	17,28	17,0
500	1,5	1,23	0,93	—	—

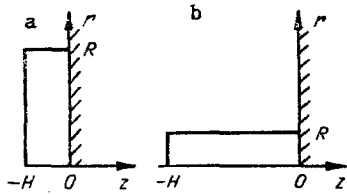


Fig. 3

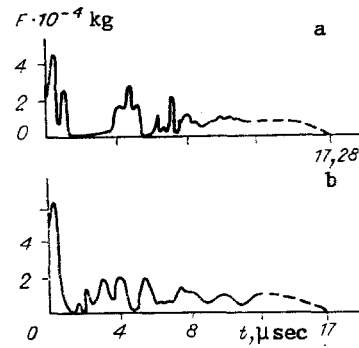


Fig. 4

propagated at identical velocity, which is related to neglecting the unloading in the pores. Let us estimate the change in the speed of sound because of unloading in the pores. The sound speed in the neighborhood of the pores will diminish from the longitudinal  $c_l$  to the core value  $c_s$ . Since the mean pore area is  $m_1$  in each section, we have for the mean speed of sound

$$\langle c \rangle_p \simeq m_1 c_s + m_2 c_l, \quad c_s = \sqrt{E/\rho}, \quad c_l = c_s \sqrt{(1-\nu)/[(1+\nu)(1-2\nu)]} \quad (2.1)$$

( $\nu$  is the Poisson ratio, and  $E$  is Young's modulus). Using (2.1) we obtain the following estimate

$$\langle c \rangle_p / c_l \simeq 1 - m_1(1 - c_s/c_l), \quad c_s/c_l = \sqrt{(1+\nu)(1-2\nu)/(1-\nu)}. \quad (2.2)$$

Setting  $\nu = 0.3$  in (2.2), we find  $c_l/\langle c \rangle_p \simeq 1.03$  for  $m_1 = 0.2$ ,  $c_l/\langle c \rangle_p \simeq 1.01$  for  $m_1 = 0.1$ . It hence follows that for a very low porosity ( $m_1 < 0.2$ ) the change in the velocity of the elastic forerunner will be small because of unloading in the pores.

3. Let us consider the problem of recoil of a cylindrical porous impactor from a solid obstacle. The mathematical problem is posed as follows: Find the functions  $u, w, \rho, \varepsilon, \sigma_{ij}, \rho_s, m_2, \rho$ , satisfying the system of equations (1.1)-(1.8), the initial conditions  $w = w_0, u = 0, \sigma_{ij} = 0, \rho = \rho_0, m_2 = m_2^0$ ; the boundary conditions  $w = 0, S_{rz} = 0$  on the contact plane ( $z = 0$ ) while  $\sigma_{ijnj} = 0$  upon standoff from the obstacle ( $z < 0$ ). The condition  $\sigma_{ijnj} = 0$  is posed on the free deforming surface of the impactor. One of the most important characteristics of the collision is the contact (collision) time  $\tau$ . The determination of  $\tau$  is performed in this paper analogously to [4]. Let us introduce the force acting on the boundary  $F(t) =$

$\int_{s(t)} \sigma_{zz}(z = 0, t) ds'$ , then the disappearance of  $F(t)$  (becoming zero) corresponds to the time

of recoil. It is natural to expect that  $\tau$  will be greater for porous impactors than for continuous. However, computations showed that this assumption is not always satisfied. The computed contact times  $\tau$  ( $\mu\text{sec}$ ) are presented in Table 1 for short and long impactors. A short impactor ( $H = 0.2$  cm,  $R = 1$  cm) is shown in Fig. 3a and a long ( $h = 1$  cm,  $R = 0.4$  cm) in Fig. 3b. Steel with the characteristics  $\rho_s^0 = 7.85$  g/cm<sup>3</sup>,  $\mu = 80$  GPa, and  $Y = 1.2$  GPa is selected as impactor material. Computations were performed for different  $w_0$  and  $m_2^0$ .

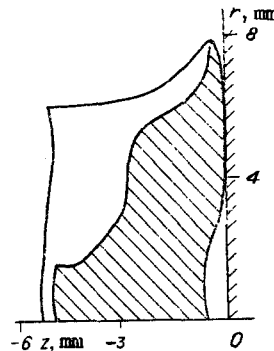


Fig. 5

It follows from Table 1 that a noticeable increase in the contact time occurs only for the short impactor. The contact times of the porous and continuous long impactors are near to each other. This latter is associated with the fact that because of side unloading waves a drop occurs in the amplitude and velocity of the plastic shockwave that occurs at the contact. Consequently, the stress is reduced by elastic waves whose propagation velocities agree for the porous and continuous impactors. The dependence  $F(t)$  is given in Fig. 4 for a long impactor for  $w_0 = 400$  m/sec. The case a corresponds to a porous impactor with  $m_2^0 = 0.9$ , and b to the continuous impactor ( $m_2^0 = 1$ ). It is seen from Fig. 4 that the force  $F$  of the porous impactor is substantially less at the initial time  $t \lesssim 2$   $\mu$ sec than for the continuous impactor. These forces are later equilibrated because of the side unloading waves. Let us note another interesting feature of the collision of porous impactors associated with the influence of the side unloading waves. As follows from (1.3), filling of the pores occurs at those points through which the plastic shock front has passed and the condition  $p > p_0$  has been satisfied. Since the shock may not reach the free surface for impactors with  $H > R$  filling of the pores in the whole impactor volume will not occur. The shading in Fig. 5 shows the domain of pore filling at the time  $t = 5$   $\mu$ sec for an impactor with  $H = 0.6$  cm,  $R = 0.5$  cm,  $w_0 = 300$  m/sec,  $m_2^0 = 0.8$ . The filling domain remains practically unchanged in the last times ( $t > 5$   $\mu$ sec). The reflected plastic wave front stands off from the obstacle a distance on the order of 3 mm and practically agrees with the boundary of the filling domain. A certain stretching of the filling domain near the axis is associated with magnification of the wave amplitude during their convergence to the axis. The influence of the side unloading can be neglected for a short impactor and the motion can be considered almost one-dimensional. In this case the shock that occurs on the contact surface reaches the free surface and is reflected by the unloading wave. The contact time is determined by the velocity of shock propagation. As has been shown in Sec. 2, the shock velocity in a porous body is substantially less than in a continuous body, consequently, the contact time is greater.

#### LITERATURE CITED

1. M. L. Wilkins and M. W. Guinan, "Cylinder impact on a rigid obstacle," *Mekhanika* [Russian translation], No. 3, Moscow (1973).
2. Kh. A. Rakhmatulin and Yu. A. Dem'yanov, *Strength under Intensive Short-range Loads* [in Russian], Fizmatgiz, Moscow (1961).
3. L. M. Kachanov, *Principles of Plasticity Theory* [in Russian], GITL, Moscow (1956).
4. A. I. Gulidov and V. M. Fomin, "Numerical modelling of the recoil of axisymmetric rods from a solid obstacle," *Zh. Prikl. Mekh. Tekh. Fiz.*, No. 3 (1980).
5. M. L. Wilkins, "Analysis of elastic-plastic flows," *Computational Methods in Hydrodynamics* [Russian translation], Mir, Moscow (1967).
6. F. A. Baum, L. P. Orlenko, K. P. Stanyukovich, et al., *Physics of Explosion* [in Russian], Nauka, Moscow (1975).
7. S. Z. Dunin and V. V. Surkov, "Effects of energy dissipation and the influence of melting on the shock compression of porous bodies," *Zh. Prikl. Mekh. Tekh. Fiz.*, No. 1 (1982).
8. Ya. B. Zel'dovich and Yu. P. Raizer, *Physics of Shockwaves and High-Temperature Hydrodynamic Phenomena* [in Russian], Nauka, Moscow (1966).
9. W. Herman, "Governing equation for the dynamic compression of plastic porous materials," *Mekhanika* [Russian translation], No. 5, Moscow (1970).